Appl. Phys. B 89, 359–365 (2007)
DOI: 10.1007/s00340-007-2796-2

Applied Physics B
Lasers and Optics

JUN DONG[1,✉]
A. SHIRAKAWA[1]
K.-I. UEDA[1]
A.A. KAMINSKII[2]

Effect of ytterbium concentration on cw Yb:YAG microchip laser performance at ambient temperature – Part I: Experiments

[1] Institute for Laser Science, University of Electro-Communications, 1-5-1 Chofugaoka, Chofu, Tokyo 182-8585, Japan
[2] Crystal Laser Physics Laboratory, Institute of Crystallography, Russian Academy of Sciences, Leninsky Pr. 59, Moscow 119333, Russia

Received: 25 April 2007 / Revised version: 6 August 2007
Published online: 21 October 2007 •

ABSTRACT The microchip laser performance of Yb:YAG crystals doped with different ytterbium concentrations ($C_{Yb} = 10$, 15, and 20 at. %) has been investigated at ambient temperature without active cooling of the gain media. Efficient laser oscillation for a 1-mm-thick YAG doped with 10 at. % Yb^{3+} ions was achieved at 1030 and 1049 nm with slope efficiencies of 85% and 81%, correspondingly. The laser performance of heavy-doped Yb:YAG crystals was limited by the thermal population at terminated lasing level and thermal lens effect at room temperature without sufficient cooling of the samples. The laser emitting spectra of Yb:YAG microchip lasers with different Yb concentrations and output couplings are addressed with the local temperature rise, due to the absorption of the pump power inside the gain media under different pump levels.

PACS 42.55.Xi; 42.70.Hj; 42.55.Rz

1 Introduction

Yttrium aluminum garnet (YAG) is an attractive laser host material because of its excellent thermal, chemical and mechanical properties [1]. Yb:YAG has been a promising candidate for high-power laser-diode (LD)-pumped solid-state lasers [2, 3]. High average output power lasers based on Yb:YAG have been achieved with high efficiency by using different laser cavity configurations, such as end-pumped microchip lasers, edge-pumped, and side-pumped laser systems [4–8]. Compared with Nd:YAG laser crystals, Yb:YAG has several advantages, such as a long storage lifetime (about 1 ms) [9, 10], a very low quantum defect (8.6% with pump wavelength of 941 nm and a laser wavelength of 1030 nm), resulting in three times less heat generation during lasing than comparable Nd-based laser systems [11]. Other advantages include a broad absorption bandwidth and less sensitivity to diode wavelength specifications [10, 12], a relatively large emission peak cross-section [13] suitable for Q-switch operation, and easy growth of high quality and moderate ytterbium contain crystals without luminescence quenching (see e.g., [14]).

✉ Fax: +81-0424-85-8960, E-mail: dong@ils.uec.ac.jp

The main disadvantage of ytterbium-doped materials is their quasi-four-level nature caused by the thermal population of terminated lasing level at $\approx 612\,cm^{-1}$ of the $^2F_{7/2}$ ground state [10]. This thermal population has deleterious effects on the resonant reabsorption of laser emission by the thermally populated terminated laser level, which contains $\approx 5\%$ of the $^2F_{7/2}$ population at room temperature (RT). The effect becomes worse at high temperature induced from the heat generated by the absorbed pump power inside the Yb:YAG crystal. In addition, the thermal population still depends strongly on the concentration of Yb^{3+} lasants in YAG crystal. Therefore, it is difficult to realize inversion population at RT; the laser threshold is high and the lasing efficiency is consequently low. There are two ways to achieve needed inversion population: by either pumping with high pump power intensities at RT or above or by depopulation of the highest Stark components of the ground state $^2F_{5/2}$. The latter can be achieved significantly by cooling Yb:YAG [10]. Efficient laser performance of Yb:YAG crystals under laser-diode pumping at cryogenic temperature has recently been demonstrated [15, 16]. The thermal conductivity of YAG decreases and the thermal loading parameter increases with increasing ytterbium concentration. Furthermore, there is strong emission quenching, which is attributed to uncontrolled impurities during crystal growth. These concentration dependent thermal properties of Yb:YAG have great unwanted effects on the laser performance of Yb:YAG microchip lasers at ambient temperature without sufficient active cooling system. The thermal conductivity, thermal expansion coefficient, and thermal loading of Yb:YAG crystals related to the temperature, temperature rise induced by the pump power deposited on the gain medium are an important factor to be considered in the laser performance of Yb:YAG at ambient temperature. Also temperature has a great impact on the emission peak cross-section of Yb:YAG crystals [13, 17]. Some of the applications require that the lasers should be compact and economic; therefore, the cooling system is eliminated in compact and easily maintainable laser system. Therefore, laser-diode end-pumped microchip lasers are a better choice to achieve highly efficient laser operation under high pump power intensity.

In this paper, we report systematically on the effect of Yb^{3+}-ion concentration on the development of Yb:YAG microchip lasers at ambient temperature. The performance of a Yb:YAG microchip laser indicated that it can be realized by

choosing the suitable Yb^{3+}-ion constant in this gain medium. The lower the ytterbium concentration, the better on the lasing of YAG crystals doped with 10, 15, and 20 at. % Yb^{3+} lasants at high pump power level. We determined that the microchip laser can oscillate efficiently at 1030 and 1049 nm with slope efficiencies of 85 and 81%, respectively, by using 1-mm-thick YAG crystals doped with 10 at. % Yb^{3+} ions. The laser properties become worse with an increase of the Yb^{3+}-ion concentration under the same thickness of Yb:YAG crystals, owing to the strong thermal population distribution in its pump area for heavy-doped Yb:YAG crystals. The laser emitting wavelength of Yb:YAG microchip lasers and switching of the emitting wavelength from 1030 nm to 1049 nm for 10 at. % Yb:YAG with 5% transmission of the output coupler was also addressed.

2 Experiments

The microchip laser experiment was carried out with a plane-parallel, 0.5 and 1-mm-thick YAG crystal plates doped with 10, 15, and 20 at. % Yb^{3+} ions as gain media. The diameter of the gain medium is 10 mm. The schematic diagram of the experimental setup is shown in Fig. 1. One surface of these plates is anti-reflection-coated at 940 nm and highly reflecting at 1030 nm to act as a cavity mirror of the laser. The other surface is anti-reflection-coated at 1030 nm lasing wavelength to reduce the cavity loss. Four plane-parallel mirrors were used as output couplers with different transmissions (T_{oc}) of 5, 10, 15, and 20% at 1.03 μm. The overall cavity length was the thickness of the gain crystal. The mechanically contacted Yb:YAG crystal and output coupler were held between two copper blocks with an aperture of 3 mm in diameter. A high power fiber-coupled 940 nm LD with a core diameter of 100 μm and numerical aperture of 0.22 was used as the pump source. Two lenses (M1 and M2) were used to focus the pump beam on the Yb:YAG crystal's rear surface and to produce a pump light footprint in the crystal of about 120 μm in diameter. About 95% of the total pumping power is incident on the Yb:YAG crystal plate after the coupling optics. The microchip lasers operated at RT without active cooling of the active element. The spectral composition of these lasers was analyzed with an optical spectrum analyzer (ANDO AQ6137).

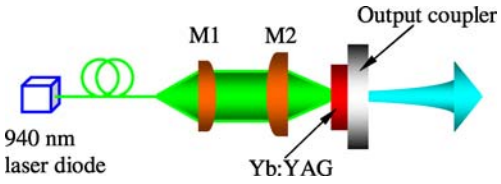

FIGURE 1 Schematic diagram of laser-diode pumped Yb:YAG microchip lasers, M1, focus lens with 8 mm focal length, M2, focus lens with 12 mm focal length

3 Results and discussion

The output power of Yb:YAG microchip lasers as a function of the absorbed pump power for $T_{oc} = 5$, 10, 15, and 20% is shown in Fig. 2. For the case of $T_{oc} = 5\%$, the absorbed pump power thresholds of 1-mm-thick microchip

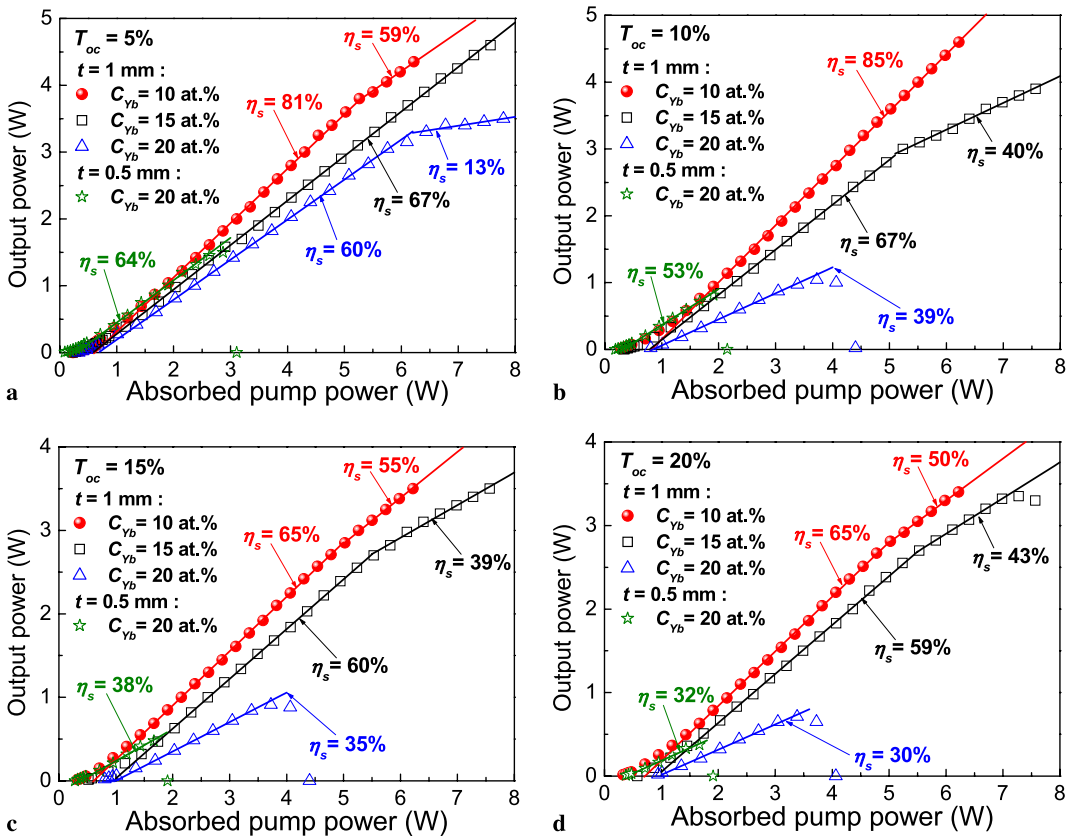

FIGURE 2 Output power of Yb:YAG microchip lasers as a function of the absorbed pump power for Yb:YAG crystals doped with different Yb^{3+} concentrations under different output coupling: (**a**) $T_{oc} = 5\%$; (**b**) $T_{oc} = 10\%$; (**c**) $T_{oc} = 15\%$; (**d**) $T_{oc} = 20\%$. The *solid lines* are the linear fits of experimental data

lasers are 0.14, 0.23, and 0.38 W for 10, 15, and 20 at. % Yb^{3+}-ion concentrations, respectively. The absorbed pump power threshold of 0.5-mm-thick Yb:YAG laser is 0.09 W for 20 at. % ytterbium concentration, which is lower than that for 1-mm-thick laser by using 20 at. % Yb:YAG as the gain medium. The output power increases linearly with the absorbed pump power when the pump power is well above the pump power threshold for Yb:YAG crystals doped with 10, 15 and 20 at. % Yb^{3+}, which is the nature of quasi-four-level operating scheme. High efficiency can be achieved by using high pump power intensity. There is a drop of the slope efficiency for 10 at. % Yb:YAG microchip laser, which is caused by the low transmission of output coupler. For 20 at. % Yb:YAG, the output power increases linearly with absorbed pump power when the absorbed pump power is lower than 6.7 W for 1-mm-thick gain medium, and output power tends to be saturated with further increase of the pump power. For 0.5-mm-thick, 20 at. % Yb:YAG crystal, the output power increases linearly with the absorbed pump power when the absorbed power is lower than 2.9 W, the laser stops with a further increase of the pump power. The interesting phenomenon for 0.5-mm-thick, 20 at. % Yb:YG microchip laser is that the output power repeats its output power when the pump power decreases from 3.2 W to its absorbed pump power threshold. This shows the performance of a 0.5-mm-thick microchip laser has a strong thermal lens effect compared to 1-mm-thick Yb:YAG microchip lasers. Maximum output power of 4.6 W was measured with 15 at. % Yb:YAG crystal as a gain medium when the absorbed pump power was 7.6 W, and the slope efficiency was about 67%, the optical-to-optical efficiency is as high as 61% with respect to absorbed pump power. The highest slope efficiency of 81% was achieved by using 10 at. % Yb:YAG crystals as the gain medium; the optical-to-optical efficiency is 70%. The output power and slope efficiency (with respect to the absorbed pump power) of 20 at. % Yb:YAG with different gain medium thickness are lower than those for the lower ytterbium concentration crystals shown in Fig. 2a and also listed in Table 1. The performance of the 0.5-mm-thick microchip laser at the available absorbed pump power range is better than that of the 1-mm-thick 20 at. % Yb:YAG. However, the maximum optical-to-optical efficiency with respect to the incident pump power ($\eta_{\text{o-o(in)}}$) of 45% was achieved with the 1-mm-thick Yb:YAG ($C_{\text{Yb}} = 20$ at. %) at incident pump power of 6.8 W, as listed in Table 1.

For $T_{\text{oc}} = 10$, 15, and 20%, the investigated lasers oscillate at 1030 nm, and the best laser performance was obtained by using $T_{\text{oc}} = 10\%$ for different Yb^{3+}-ion concentrations in YAG crystals (as shown in Fig. 2b–d). The slope efficiencies are 85, 67, and 39% for 1-mm-thick YAG doped with 10, 15, and 20 at. % Yb^{3+}-ions, and the optical-to-optical efficiencies are 74, 57, and 29%, with respect to the absorbed pump power. With 0.5-mm-thick 20 at. % Yb:YAG doped as a gain medium, the slope efficiency of 53% is higher than that for the 1-mm-thick 20 at. % Yb:YAG laser, and the corresponding optical-to-optical efficiency is 43% with respect to the absorbed pump power. A maximum output power of 4.6 W was achieved with 10 at. % Yb:YAG as a gain medium. The output power of the 10 at. % Yb:YAG microchip laser increases linearly with the absorbed pump power. For 15 at. % Yb:YAG, the output power tends to increase slowly with absorbed pump power when the absorbed pump power is higher than 5.4 W (slope efficiency decreases from 67% to 40%). For 20 at. % Yb:YAG, even with different thicknesses (0.5 and 1 mm), there is a maximum absorbed pump power, when the pump power is higher than this value (4.5 W for 1-mm-thick Yb:YAG and 2.2 W for 0.5-mm-thick Yb:YAG), there is no lasing. However, when the absorbed pump power decreases again, the output power is the same as that obtained when the absorbed pump power increases to such a value. The process is reversible. Such phenomenon suggests there is strong thermal effect on the heavy-doped Yb:YAG crystals; such results are coincident with the Yb^{3+} concentration dependent

Yb:YAG	T_{oc} (%)	λ_{L} (nm)	P_{th} (W)	P_{abs} (W)	P_{out} (W)	η_{slope} (%)	$\eta_{\text{o-o(a)}}$ (%)	$\eta_{\text{o-o(in)}}$ (%)
10 at. %, 1 mm thick	5	1030						
		1030 + 1049	0.14	5.3	4.35	81	72	43
		1049						
	10	1030	0.21	6.2	4.6	85	74	44
	15	1030	0.27	5.3	3.5	65	57	34
	20	1030	0.35	5.0	3.4	65	56	33
15 at. %, 1 mm thick	5	1049	0.23	7.3	4.6	67	61	44
	10	1030	0.34	5.2	3.9	67	57	41
	15	1030	0.46	5.5	3.5	60	49	36
	20	1030	0.58	5.5	3.3	59	49	36
20 at. %, 1 mm thick	5	1049	0.38	5.8	3.5	60	53	45
	10	1030	0.6	3.4	1.04	39	29	24
	15	1030	0.7	3.4	0.9	35	25	21
	20	1030	0.87	3.0	0.71	30	21	18
20 at. %, 0.5 mm thick	5	1049	0.09	2.1	1.5	64	56	33
	10	1030	0.19	1.7	0.81	53	43	26
	15	1030	0.28	1.4	0.48	38	29	17
	20	1030	0.38	1.4	0.38	32	23	14

TABLE 1 Performance of Yb:YAG microchip lasers with different Yb^{3+} lasants. λ_{L}, laser emitting wavelength; P_{abs}, absorbed pump power at maximum optical-to-optical efficiency; P_{out}, maximum output power; $\eta_{\text{o-o(a)}}$, maximum optical-to-optical efficiency corresponding to absorbed pump power; $\eta_{\text{o-o(in)}}$, maximum optical-to-optical efficiency corresponding to incident pump power

thermal conductivity and thermal loading data for Yb:YAG crystals [14]. For $T_{oc} = 15$, and 20%, all analogous parameters for Yb:YAG microchip lasers with different concentrations and thickness (as shown in Fig. 2c for $T_{oc} = 15\%$ and Fig. 2d for $T_{oc} = 20\%$) were worse than those for $T_{oc} = 5$, and 10% (as shown in Fig. 2a for $T_{oc} = 5\%$ and Fig. 2b for $T_{oc} = 10\%$).

Figure 3 shows the optical-to-optical efficiencies with respect to the absorbed pump power of Yb:YAG microchip lasers as a function of the absorbed pump power for different Yb^{3+}-ion concentrations under different output couplings. Under the present pump power level (available incident pump power of 10 W), there is no saturation effect only for 10 at. % Yb:YAG with $T_{oc} = 10\%$ although the optical efficiency increases slowly with the absorbed pump power (as shown in Fig. 3b), maximum optical-to-optical efficiency of 74% was achieved at the absorbed pump power of 6.2 W. However, there is saturation effect of Yb:YAG microchip lasers under other different conditions. Maximum optical efficiency of 72% with $T_{oc} = 5\%$ (1049 nm lasing emitting wavelength) was achieved at the absorbed pump power of 5.3 W for 1-mm-thick Yb:YAG crystal doped with 10 at. % Yb; and optical efficiency decreases with a further increase of the absorbed pump power (see Fig. 3a). The causes of the saturation effect are thermal-induced strong reabsorption at terminated lasing level and strong thermal lens effect in the gain medium. The decrease of the optical efficiency with Yb concentration for 1-mm-thick microchip lasers was caused by the increase of the thermal population at the terminated lasing level and the thermal lens effect. Although optical efficiency for thin (0.5-mm-thick) 20 at. % Yb:YAG microchip lasers is higher than those for 1-mm-thick YAG doped with 20 at. % Yb^{3+}-ions, the serious heat generated in thin gain medium is the main factor to limit the laser performance at room temperature without sufficient cooling for the samples. Maximum optical-to-optical efficiency with respect to the absorbed pump power and incident pump power under different laser working conditions are also listed in Table 1.

The laser spectra of our microchip lasers indicate several longitudinal modes oscillate simultaneously. For the case with $T_{oc} = 5\%$, four longitudinal modes oscillate at 1030 nm under just over threshold pump power, while six longitudinal modes oscillate with further increase of pump power when absorbed pump power is kept lower than 0.55 W for 10 at. % Yb:YAG microchip laser, as shown in Fig. 4a. Dual-wavelength (1030 and 1049 nm) oscillation of a 10 at. % Yb:YAG laser was observed when the absorbed pump power was kept between 0.55 and 0.75 W. The intensity and number of longitudinal modes at 1030 nm decrease and the number of longitudinal modes around 1049 nm increases with increasing pump intensity. The 10 at. % Yb:YAG microchip laser

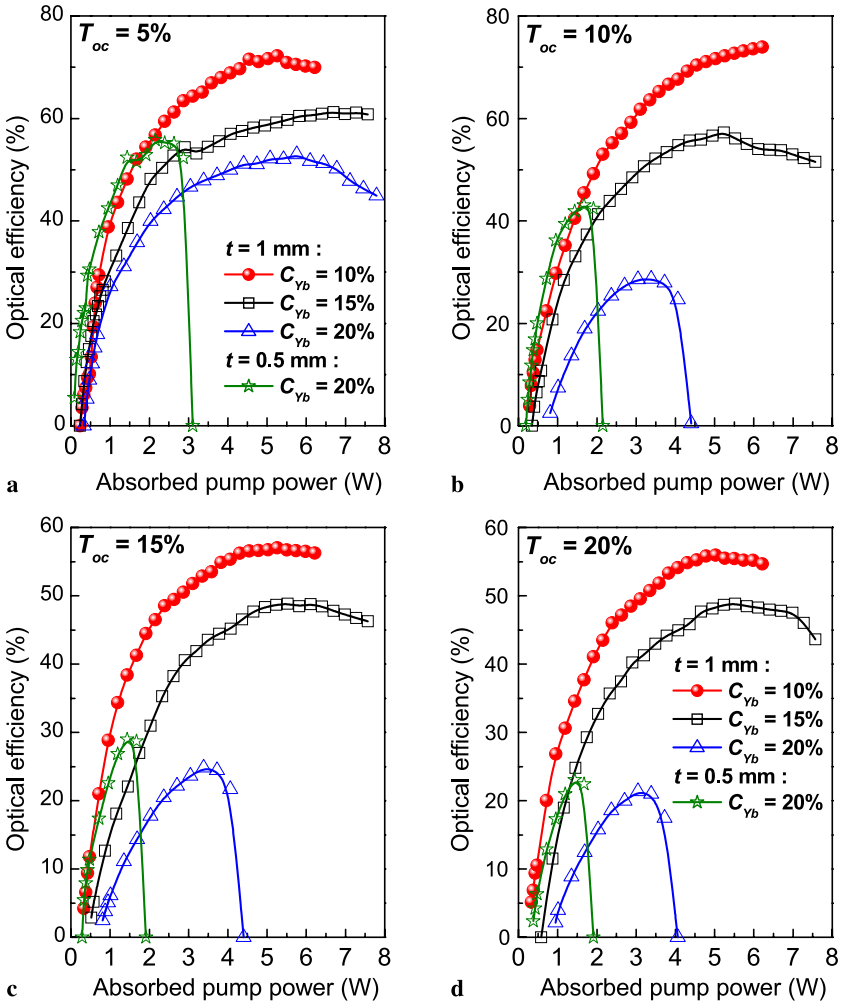

FIGURE 3 Optical-to-optical efficiency of Yb:YAG microchip lasers as a function of the absorbed pump power for Yb:YAG crystals doped with different Yb^{3+} concentrations under different output couplings

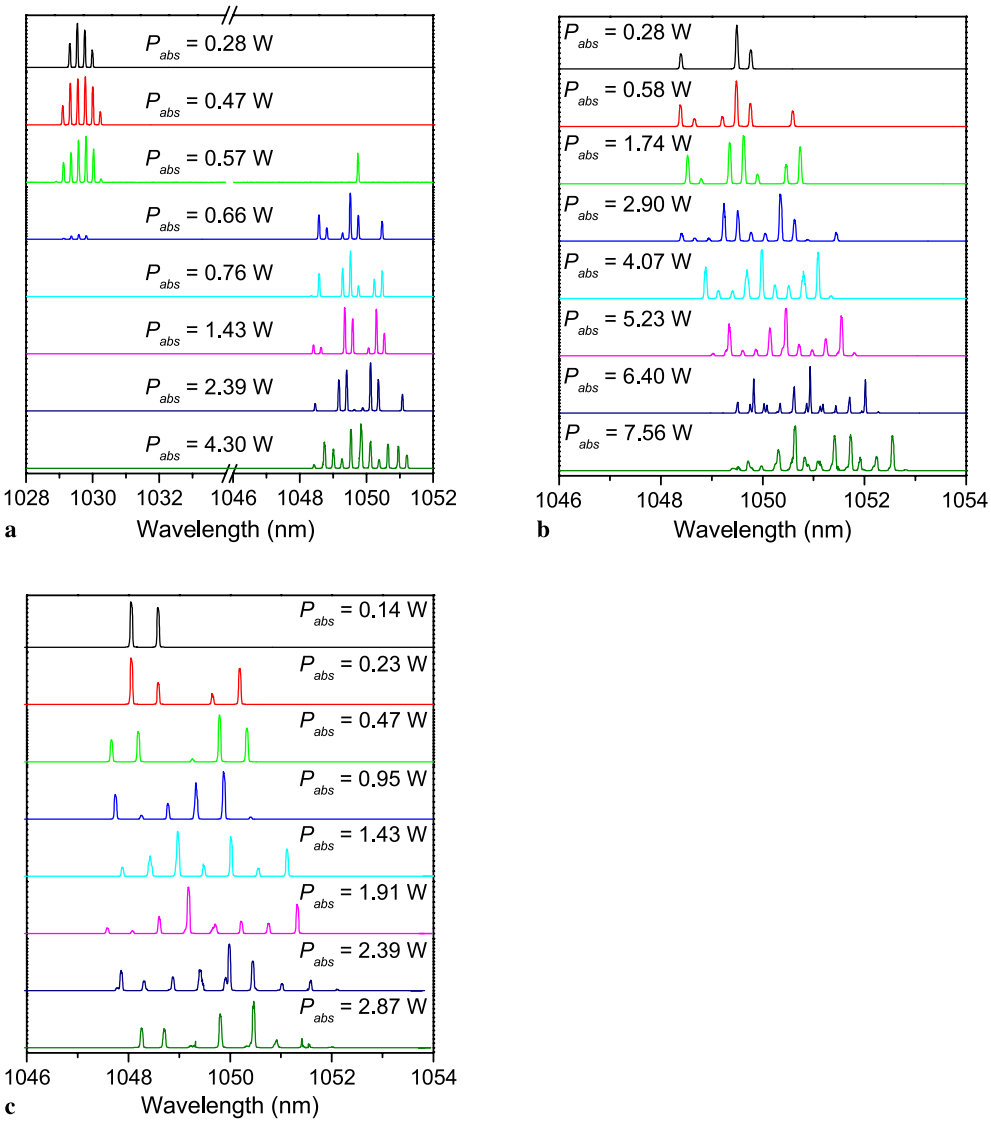

FIGURE 4 Laser spectra of Yb:YAG microchip lasers for $T_{oc} = 5\%$, (**a**) 1 mm thick, 10 at. % Yb:YAG, (**b**) 1 mm thick, 15 at. % Yb:YAG, (**c**) 0.5 mm thick, 20 at. % Yb:YAG

oscillates around 1049 nm when the absorbed pump power is above 0.75 W. The longitudinal modes around 1049 nm increase with absorbed pump power (as shown in Fig. 4a). For YAG crystals doped with higher concentrations of Yb^{3+} ions ($C_{Yb} = 15$ and 20 at. %), the laser operates at 1049 nm only for $T_{oc} = 5\%$, because of the strong reabsorption of Yb^{3+}-ions at 1030 nm. Figure 4b shows the laser emitting spectra of 15 at. % Yb:YAG laser under different pump power levels. The number of the longitudinal mode increases from three to twelve, and oscillating emission shifts to longer wavelength with the pump power. In addition, strong mode competition and mode hopping were observed for 1049 nm laser operation. Figure 4c shows the laser spectra of 0.5-mm-thick, 20 at. % Yb:YAG laser under different pump power levels. The number of the longitudinal mode increases from two to eight with the pump power.

For the case of $T_{oc} = 10$, 15, and 20%, Yb:YAG microchip lasers operate at around 1030 nm, owing to the increase of the output coupling, the loss increases and the gain provided at 1049 nm is lower than that at 1030 nm and can not overcome the loss of large output coupling; therefore, the laser oscillates at shorter wavelength. Figure 5 shows the emission spectra of 1-mm-thick lasers with Yb:YAG crystals doped with 10 and 15 at. % Yb^{3+} ions, and 0.5-mm-thick laser with 20 at. % Yb:YAG crystal for $T_{oc} = 10\%$. The number of longitudinal modes of 10 at. % Yb:YAG laser increase from three to eight with the pump power, as shown in Fig. 5a. The number of longitudinal modes of the 15 at. % Yb:YAG laser increases from five to ten with the pump power; also the longitudinal mode at high pump power tends to bifurcate, as shown in Fig. 5b. The number of longitudinal modes increases from three to six with the absorbed pump power for 0.5-mm-thick 20 at. % Yb:YAG laser, as shown in Fig. 5c. The laser emission shifts to longer wavelengths with pump power, and the shift of the wavelength become strong with an increase of the pump power. The shift of laser emission to longer wavelengths increases with increasing Yb^{3+}-ion concentration in YAG crystals due to the more severe heat generation arising in lasing Yb:YAG crystals [13]. The laser oscillation thresholds at 1030 nm and 1049 nm for Yb:YAG microchip lasers are governed by the gain provided at 1030 nm or 1049 nm and the total losses including the useful output coupling loss, the intracavity loss

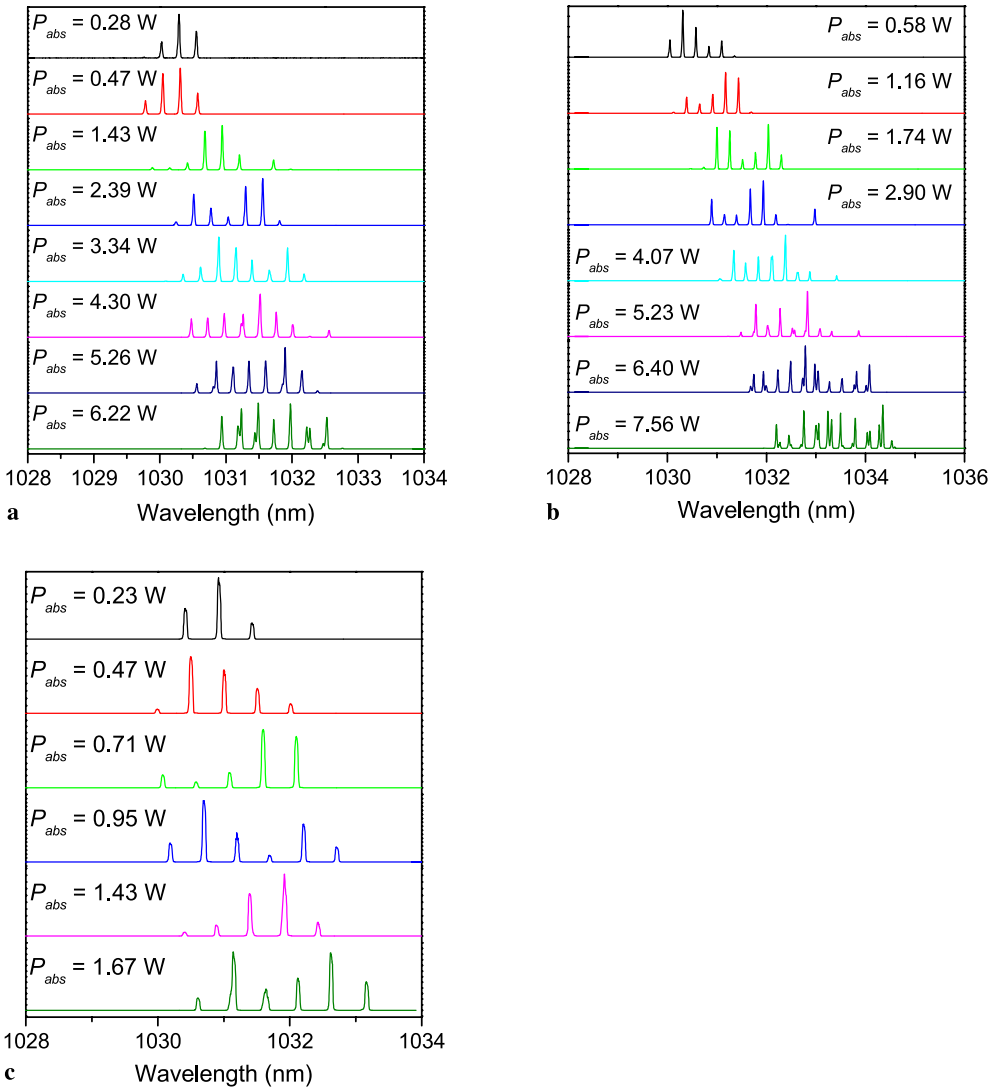

FIGURE 5 Laser spectra of Yb:YAG microchip lasers for $T_{oc} = 10\%$, (**a**) 1 mm thick, 10 at. % Yb:YAG, (**b**) 1 mm thick, 15 at. % Yb:YAG, (**c**) 0.5 mm thick, 20 at. % Yb:YAG

and the reabsorption loss. The gain provided at 1030 nm is larger than that provided at 1049 nm because the emission peak cross-section at 1030 nm is five times higher than that at 1049 nm for Yb:YAG crystal. However, the reabsorption loss at 1030 nm is larger than that at 1049 nm for Yb:YAG crystal. The reabsorption loss is proportional to the Yb^{3+}-ion concentrations, and temperature dependent thermal population distribution factor of terminated laser level of Yb:YAG crystal. With the same intracavity loss at both wavelengths, the transmission of the output coupler is the main factor for controlling the laser emitting wavelength. For $T_{oc} = 5\%$ or less, the net gain at 1030 nm owing to the strong reabsorption is smaller than that at 1049 nm. The laser prefers to oscillate at 1049 nm. Otherwise, the net gain at 1030 nm is larger than that at 1049 nm for $T_{oc} = 10\%$ or high, the laser prefers oscillated at 1030 nm.

The cause of the change of laser wavelength and dual-wavelength operation for 10 at. % Yb:YAG microchip laser with $T_{oc} = 5\%$ is attributed to the quasi-four level nature of Yb:YAG and the local temperature rise due to the heat generated at high pump power. The local temperature rising inside Yb:YAG has a great effect on the thermal population distribution of terminated laser level for 1030 nm. Therefore the reabsorption around the strong emission peak of 1030 nm increases, the threshold for 1030 nm oscillation increases; however, the local temperature rise has little effect on the reabsorption loss around the weak emission peak of 1049 nm for Yb:YAG crystal; there is a tradeoff between 1030 and 1049 nm lasing. With a further increase of the local temperature, the laser prefers to oscillate at 1049 nm rather than at 1030 nm with $T_{oc} = 5\%$. Therefore, when the absorbed pump power is higher than a certain value, the laser oscillates at 1049 nm. For heavy-doped Yb:YAG crystals ($C_{Yb} = 15$ and 20 at. %), the reabsorption loss plays an important role in the laser oscillation threshold; the laser prefers to oscillate at 1049 nm rather than at 1030 nm for $T_{oc} = 5\%$.

For the case of 1-mm-thick Yb:YAG microchip lasers, the separation of two close longitudinal modes was measured to be 0.3 nm for 1049 nm oscillation. The wide separation between these modes clearly shows that there is strong mode hopping and mode-competition between longitudinal modes around 1049 nm. This may be caused by flatter emission spectra around 1049 nm than around 1030 nm for Yb:YAG crystal [13] and the gain distribution along the Fabry–Pérot

resonator. The separation of each longitudinal mode under different pump power was about 0.29 nm for 1030 nm oscillation. The separation between each mode was measured to be 0.58 nm for 0.5-mm-thick Yb:YAG microchip laser, which is two times of that for 1-mm-thick Yb:YAG microchip lasers. The separation of the longitudinal modes in a laser cavity was given by [18] $\Delta\lambda = \lambda^2/(2L_c)$, where L_c is the optical length of the resonator, λ is the laser emitting wavelength. For 1-mm-thick plane-parallel Yb:YAG gain medium studied here, $\Delta\lambda$ was calculated to be 0.2915 and 0.302 nm with the laser wavelength of 1030 and 1049 nm, respectively, which were in good agreement with the experimental data. For 0.5-mm-thick plane-parallel Yb:YAG gain medium, $\Delta\lambda$ was calculated to be 0.583 and 0.604 nm with the laser wavelength of 1030 and 1049 nm, respectively, which were also in good agreement with the experimental data. The linewidth at each mode was measured to be less than 5.7 GHz, i.e., the resolution limit of the used instrument.

4 Conclusions

In conclusion, microchip laser performance has been investigated systematically by adopting YAG crystals doped with different Yb^{3+}-ion concentrations at ambient temperature without active cooling of the gain media. Efficient laser performance of at 1030 and 1049 nm was achieved by using 10 at. % Yb:YAG crystals; the slope efficiency with respect to the absorbed pump power of 85% and 81% was achieved for 1030 and 1049 nm oscillations. Dual-wavelength (1030 and 1049 nm) lasing can be achieved by using 10 at. % Yb:YAG crystal and $T_{oc} = 5\%$ output coupler in a narrow pump power range. The laser performance of the Yb:YAG microchip lasers at 1030 nm oscillation is strongly affected by the Yb concentration, becoming worse with an increase of the Yb^{3+}-ion concentration in YAG crystals at ambient temperature, because the thermal properties of heavy-doped Yb:YAG crystal are getting worse and reabsorption loss is large. However, the laser performance of Yb:YAG microchip lasers working at 1049 nm is nearly independent of Yb concentration for 1-mm-thick Yb:YAG crystals with respect to the incident pump power. The strong thermal lens effect limits the laser performance of Yb:YAG microchip lasers for heavy-doped Yb:YAG crystals.

ACKNOWLEDGEMENTS This work was supported by the 21st Century Center of Excellence (COE) program of Ministry of Education, Science, Sports, and Culture of Japan. One of us (A.A.K.) wishes to acknowledge the Russian Foundation for Basic Research.

REFERENCES

1 A.A. Kaminskii, *Laser Crystals* (Springer, Berlin Heidelberg New York, 1981)
2 A. Giesen, H. Hugel, A. Voss, K. Wittig, U. Brauch, H. Opower, Appl. Phys. B **58**, 365 (1994)
3 T.S. Rutherford, W.M. Tulloch, E.K. Gustafson, R.L. Byer, IEEE J. Quantum Electron. **QE-36**, 205 (2000)
4 E.C. Honea, R.J. Beach, S.C. Mitchell, J.A. Sidmore, M.A. Emanuel, S.B. Sutton, S.A. Payne, P.V. Avizonis, R.S. Monroe, D. Harris, Opt. Lett. **25**, 805 (2000)
5 C. Stewen, K. Contag, M. Larionov, A. Giessen, H. Hugel, IEEE J. Sel. Top. Quantum Electron. **6**, 650 (2000)
6 M. Tsunekane, T. Taira, Opt. Lett. **31**, 2003 (2006)
7 Q. Liu, M. Gong, F. Lu, W. Gong, C. Li, D. Ma, Appl. Phys. Lett. **88**, 101 113 (2006)
8 H. Bruesselbach, D.S. Sumida, IEEE J. Sel. Top. Quantum Electron. **11**, 600 (2005)
9 D.S. Sumida, T.Y. Fan, Opt. Lett. **19**, 1343 (1994)
10 G.A. Bogomolova, D.N. Vylegzhanin, A.A. Kaminskii, Sov. Phys. JETP **42**, 440 (1976)
11 T.Y. Fan, IEEE J. Quantum Electron. **QE-29**, 1457 (1993)
12 H.W. Bruesselbach, D.S. Sumida, R.A. Reeder, R.W. Byren, IEEE J. Sel. Top. Quantum Electron. **3**, 105 (1997)
13 J. Dong, M. Bass, Y. Mao, P. Deng, F. Gan, J. Opt. Soc. Am. B **20**, 1975 (2003)
14 F.D. Patel, E.C. Honea, J. Speth, S.A. Payne, R. Hutcheson, R. Equall, IEEE J. Quantum Electron. **QE-37**, 135 (2001)
15 D.J. Ripin, J.R. Ochoa, R.L. Aggarwal, T.Y. Fan, Opt. Lett. **29**, 2154 (2004)
16 S. Tokita, J. Kawanaka, M. Fujita, T. Kawashima, Y. Izawa, Appl. Phys. B **80**, 635 (2005)
17 D.S. Sumida, T.Y. Fan, In: *Advanced Solid-State Lasers*, ed. by T.Y. Fan, B.H.T. Chai (Optical Society of America, Washington, D.C., 1994), Vol. 20, p. 100
18 W. Koechner, *Solid State Laser Engineering* (Springer, Berlin, 1999)